Phosphonate-functionalized heteroleptic ruthenium(II) bis(2,2':6',2''-terpyridine) complexes

Edwin C. Constable,* Catherine E. Housecroft,* Markéta Šmídková and Jennifer A. Zampese

Department of Chemistry, University of Basel, Spitalstrasse 51, CH-4056 Basel, Switzerland

This paper is dedicated to our colleague Barry Lever whose contributions to inorganic chemistry have extended over a long and distinguished career.

Abstract

The heteroleptic complexes [Ru(**1**)(**4**)][PF_6]$_2$, [Ru(**2**)(**4**)][PF_6]$_2$, [Ru(Phtpy)(**4**)][PF_6]$_2$ and [Ru(pytpy)(**4**)][PF_6]$_2$ (Phtpy = 4'-phenyl-2,2':6',2''-terpyridine, pytpy = 4'-(4-pyridyl)-2,2':6',2''-terpyridine, **1** and **2** = 4-methyl ester-substituted derivatives of Phtpy and pytpy, **4** = ethyl 2,2':6',2''-terpyridine-4'-phosphonate) have been prepared. The single crystal structure of ligand **1** (**1** = methyl 4-carboxy-4'-phenyl-2,2':6',2''-terpyridine) is reported. The introduction of the 4-methyl ester group causes a small red shift in the MLCT band of the ruthenium(II) complexes, and small shift to more positive potential for the Ru^{2+}/Ru^{3+} couple. The new

complexes should serve as a useful starting point for development of ruthenium(II) dyes suited for sensitization of p-type semiconductors.

Introduction

The {Ru(tpy)$_2$} chromophore (tpy = 2,2':6',2''-terpyridine) is one of the most extensively studied domains[1] within metal oligopyridine coordination chemistry. Tuning the photophysical and electrochemical properties of {Ru(tpy)$_2$}-containing complexes is readily achieved through functionalization of the ligand. In particular, the Kröhnke methodology[2] is a facile means of introducing a wide variety of substituents into the 4'-position of tpy. Although at room temperature in solution, [Ru(tpy)$_2$]$^{2+}$ is essentially non-emissive,[3] judicious choice of electron-donating or accepting substituents can lead to significant enhancement of emission properties.[4]

Among the many areas in which ruthenium(II) complexes containing tpy-derived ligands have found a practical niche is that of the Grätzel solar cell.[5] Our own interests in the development of sensitizers for the photoanode in dye-sensitized solar cells (DSCs) have moved in the direction of earth-abundant metals, in particular copper.[6] Although photon-to-power conversion efficiencies reaching 3.77%[7] have been achieved with a copper(I) sensitizer anchored to the n-type semiconductor (TiO_2) comprising the photoanode, this is significantly lower than those attained by state-of-the-art ruthenium(II) dyes (>10%).[8] One strategy for improving performance is to harvest photons at both electrodes, but this requires different dyes suited for interaction with either the photoanode (n-type

semiconductor) or photocathode (p-type) in a so-called tandem cell.[9] In a tandem DSC, the photocathode functions in an inverse mode with respect to the photoanode, with excitation of the dye being followed by rapid hole injection into the p-type semiconductor (e.g. NiO). Organic donor–acceptor molecules are popular choices for photocathode sensitizers.[10] Excitation of the sensitizer leaves a hole in the original HOMO of the dye into which an electron is transferred from the valence band of the p-type semiconductor. Thus, the HOMO/LUMO requirements of a p-type sensitizer are the reverse of those of an n-type dye. It has been demonstrated that $[Ru(bpy)_2(N^N)]^{2+}$ (bpy = 2,2'-bipyridine, N^N = bipyridine-based anchoring ligand) complexes sensitize NiO photocathodes and both CO_2H and $PO(OH)_2$ anchors adsorb onto NiO.[11] Ruthenium(II) complexes containing cyclometalated ligands, and related to the archetypal $[Ru(bpy)_2(ppy)]^+$ [12,13] (Hppy = 2-phenylpyridine) are also promising candidates for NiO sensitization.[14,15]

Low level MO calculations indicate that the HOMO of $[Ru(tpy)(4'-(HO)_2OPtpy)]^{2+}$ type complexes (4'-$(HO)_2$OPtpy = 2,2':6',2''-terpyridine-4'-phosphonic acid) may be localized on the phosphonic acid anchoring unit. We have therefore undertaken a preliminary investigation of several complexes of this type with the aim of provding a starting point for the development of dyes for p-type semiconductors. The ancillary ligands **1** and **2** (Scheme 1) contain an ester functionality which provides a site for variable functionalization, for example, through transesterification.

Experimental

General: ^{1}H and ^{13}C NMR spectra were recorded at 295 K on Bruker Avance III-400 or III-500 NMR spectrometers (chemical shifts with respect to residual solvent peaks and ∂(TMS) = 0 ppm). Solution electronic absorption and emission spectra were measured, respectively, using an Agilent 8453 spectrophotometer and Shimadzu 5301PC spectrofluorophotometer. Solution quantum yields were measured using a Hamamatsu absolute PL quantum yield spectrometer C11347 Quantaurus_QY. A Shimadzu 8400S spectrometer was used to record FT-IR spectra (all solid samples using a Golden Gate accessory). Electrospray ionization (ESI) mass spectra and high-resolution ESI mass spectra were recorded on Bruker esquire 3000^{plus} and Bruker maXis 4G mass spectrometers. Electrochemical measurements were carried out using cyclic voltammetry and were recorded using a CH Instruments 900B potentiostat with glassy carbon working and platinum auxiliary electrodes; a silver wire was used as a pseudo-reference electrode. The solvent was HPLC grade MeCN and 0.05 M $[^{n}Bu_4N][PF_6]$ was used as supporting electrolyte. All solutions were degassed with argon, and Cp_2Fe was used as internal reference. A Biotage Initiator 8 reactor was used for reactions under microwave conditions. Fluka silica 60 was used for column chromatography.

The compounds (*E*)-1-(pyridin-2-yl)-3-(pyridin-4-yl)prop-2-en-1-one,[16] (*E*)-3-phenyl-1-(pyridin-2-yl)prop-2-en-1-one,[17] 1-(2-(4-(methoxycarbonyl)pyridin-2-yl)-2-oxoethyl)pyridin-1-ium iodide,[16] Phtpy[17] pytpy[18] and 4'-F_3CSO_3-2,2':6',2''-terpyridine[19] were prepared according to published methods (Phtpy = 4'-phenyl-2,2':6',2''-terpyridine, pytpy = 4'-(4-pyridyl)-2,2':6',2''-terpyridine). $RuCl_3 \cdot 3H_2O$ was purchased from OXKEM.

Compound 1

Ammonium acetate (9.60 g, 124.68 mmol) was dissolved in MeOH (110 mL). (*E*)-3-Phenyl-1-(pyridin-2-yl)prop-2-en-1-one (1.00 g, 4.76 mmol) and 1-(2-(4-(methoxycarbonyl)pyridin-2-yl)-2-oxoethyl)pyridin-1-ium iodide (2.21 g, 5.71 mmol) were added and the brown solution was heated at reflux for 16 h, during which time a brown precipitate formed. The reaction mixture was then cooled to room temperature and left to stand overnight in a freezer. The brown precipitate was collected on a glass frit, washed with cold MeOH and dried in air. Compound **1** was isolated as a pale brown powder (0.56 g, 1.53 mmol, 33%). M.Pt. 197-198 °C. ^{1}H NMR (500 MHz, $CDCl_3$) ∂/ppm 9.16 (dd, J = 1.7, 0.9 Hz, 1H, H^{D3}), 8.86 (dd, J = 5.0, 0.9 Hz, 1H, H^{D6}), 8.78 (d, J = 1.7 Hz, 1H, H^{B3}), 8.75 (d, J = 1.7 Hz, 1H, H^{B5}), 8.74 (ddd, J = 4.7, 1.9, 1.0 Hz, 1H, H^{A6}), 8.72 (dt, J = 7.9, 1.1 Hz, 1H, H^{A3}), 7.90 (m, 4H, $H^{A4+C2+D5}$), 7.52 (m, 2H, H^{C3}), 7.47 (m, 1H, H^{C4}), 7.37 (ddd, J = 7.5, 4.8, 1.2 Hz, 1H, H^{A5}), 4.04 (s, 3H, H^{OMe}). ^{13}C {^{1}H} NMR (126 MHz, $CDCl_3$) ∂ / ppm 166.1 ($C^{C=O}$), 157.6 (C^{D2}), 156.2 (C^{A2}), 156.1 (C^{B2}), 155.3 (C^{B6}), 150.6 (C^{B4}), 150.0 (C^{D6}), 149.2 (C^{A6}), 138.5 (C^{C1}), 138.4 (C^{D4}), 137.2 (C^{A4}), 129.3 (C^{C4}), 129.1 (C^{C3}), 127.5 (C^{C2}), 124.1 (C^{A5}), 122.9 (C^{D5}), 121.7 (C^{A3}), 120.8 (C^{D3}), 119.5 (C^{B5}), 119.3 (C^{B3}), 52.9 (C^{OMe}). ESI-MS (MeOH/$CHCl_3$): *m/z* 390.0 $[M+Na]^+$ (calc. 390.1), 368.0 $[M+H]^+$ (base peak, calc. 368.1). IR (solid, ν/cm^{-1}) 3051 (w), 2969 (w), 1723 (s), 1583 (m), 1548 (m), 1467 (w), 1432 (m), 1378 (s), 1268 (s), 1218 (s), 1132 (w), 1099 (w), 989 (m), 887 (w), 800 (m), 775 (m), 764 (s), 754 (s), 731 (s), 707 (s), 694 (s), 681 (s), 662 (s), 620 (s), 517 (s). UV/VIS λ/nm (CH_3CN, 4.44×10^{-5} mol dm^{-3}) (ε / dm^3 mol^{-1} cm^{-1}) 253

(35000), 276 sh (27000), 310 sh (13000). Found C, 74.41; H, 4.67; N, 11.22; $C_{23}H_{17}N_3O_2 \cdot 0.25H_2O$ requires C, 74.28; H, 4.74; N, 11.30%.

Compound 2

Ammonium acetate (13 g, 160 mmol) was dissolved in MeOH (150 mL). (*E*)-1-(Pyridin-2-yl)-3-(pyridin-4-yl)prop-2-en-1-one (0.92 g, 4.38 mmol) and 1-(2-(4-(methoxycarbonyl)pyridin-2-yl)-2-oxoethyl)pyridin-1-ium iodide (2.01 g, 5.25 mmol) were added and the brown suspension was heated at reflux for 7 h; the solids slowly dissolved. The white precipitate which formed was collected on a glass frit, washed with cold MeOH and Et_2O, and dried in air. Compound **2** was isolated as a white powder (1.43 g, 3.88 mmol, 89%). M.Pt. 216-217 °C. ^{1}H NMR (500 MHz, $CDCl_3$) ∂/ppm 9.15 (dd, J = 1.6, 0.9 Hz, 1H, H^{D3}), 8.86 (dd, J = 5.0, 0.9 Hz, 1H, H^{D6}), 8.78 (d, J = 1.7 Hz, 1H, H^{B3}), 8.76 (m, 3H, H^{C2+B5}), 8.72 (m, 2H, H^{A6+A3}), 7.92 (m, 2H, H^{A4+D5}), 7.80 (dd, J = 4.5, 1.7 Hz, 2H, H^{C3}), 7.39 (ddd, J = 7.5, 4.8, 1.3 Hz, 1H, H^{A5}), 4.04 (s, 3H, H^{OMe}). ^{13}C {^{1}H} NMR (126 MHz, $CDCl_3$) ∂/ppm 165.9 ($C^{C=O}$), 156.9 (C^{D2}), 156.7 (C^{B2}), 155.6 (C^{B6}), 155.5 (C^{A2}), 150.6 (C^{C2}), 150.0 (C^{D6}), 149.3 (C^{A6}), 147.6 (C^{B4}), 145.9 (C^{C4}), 138.5 (C^{D4}), 137.2 (C^{A4}), 124.3 (C^{A5}), 123.2 (C^{D5}), 121.7 (C^{C3}), 121.6 (C^{A3}), 120.7 (C^{D3}), 119.1 (C^{B3}), 118.9 (C^{B5}), 53.0 (C^{OMe}). ESI MS (MeOH/$CHCl_3$): m/z 391.1 $[M+Na]^+$ (base peak, calc. 391.1), 369.2 $[M+H]^+$ (calc. 369.1). IR (solid, ν/cm^{-1}) 3020 (w), 2961 (w), 1731 (s), 1583 (m), 1559 (m), 1538 (m), 1533 (m), 1475 (m), 1436 (m), 1378 (m), 1309

(w), 1292 (w), 1270 (m), 1263 (w), 1218 (m), 1211 (m), 1130 (w), 973 (w), 895 (w), 821 (m), 795 (s), 770 (s), 736 (w), 682 (m), 669 (m), 660 (m), 618 (m), 533 (m). UV/VIS λ/nm (ε / $dm^3\ mol^{-1}\ cm^{-1}$) (CH_3CN, 4.22×10^{-5} mol dm^{-3}) 242 (33000), 281 (16000), 316 sh (10000). Found C, 70.96; H, 4.44; N, 15.19; $C_{22}H_{16}N_4O_2 \cdot 0.25H_2O$ requires C, 70.86; H, 4.46; N, 15.02%.

Compound 3

4'-F_3CSO_3-2,2':6',2''-Terpyridine (0.80 g, 2.10 mmol) and [$Pd(PPh_3)_4$] (0.24 g, 0.21 mmol) were suspended in MeCN (17 mL) in a microwave vial (20 mL), and then NEt_3 (0.38 g, 3.78 mmol) and diethyl phosphite (0.49 g, 3.57 mmol) were added. The brown suspension was heated in a microwave reactor (140 °C, 30 min) and then allowed to cool to room temperature. The reaction mixture was diluted with toluene and washed with aqueous NH_4OH (32%) and H_2O. The organic layer was dried over $MgSO_4$, filtered and the solvent removed in vacuo. The crude brown solid was purified by flash column chromatography (SiO_2), first eluting with CH_2Cl_2 to remove Ph_3PO and then with CH_2Cl_2/MeOH (98 : 2). Compound **3** was isolated as a pale brown solid (0.65 g, 1.76 mmol, 84%). The NMR spectroscopic data matched those published.[20]

[Ru(3)Cl_3]

Compound **3** (0.60 g, 1.63 mmol) and $RuCl_3 \cdot 3H_2O$ (0.43 g, 1.63 mmol) were suspended in EtOH (200 mL) and the reaction mixture was heated at reflux for 3.5 h. The brown solid which formed was separated by filtration, washed with cold EtOH and Et_2O and dried in air yielding a red-brown powder (0.83

g, 1.44 mmol, 88%). The product was used for the next step without further purification and characterization.

[Ru(Phtpy)(4)][PF_6]$_2$

Phtpy (64 mg, 0.21 mmol) and [Ru(**3**)Cl_3] (119 mg, 0.21 mmol) were suspended in dry EtOH (3.5 mL) in a microwave reactor vial. *N*-Ethylmorpholine (3 drops) was added and the reaction mixture was heated in a microwave reactor at 140 °C for 15 min. The dark red solution was poured into aqueous NH_4PF_6 (250 mL) yielding a red precipitate which was collected on Celite and washed with cold water (250 mL) and Et_2O (20 mL). The residue was redissolved in CH_3CN and then solvent removed in vacuo to give a dark red solid. This was purified by column chromatography (SiO_2, eluted with CH_3CN/saturated aqueous KNO_3/H_2O 7 : 1 : 0.5 by vol.). The first red band was collected, aqueous NH_4PF_6 added and solvent evaporated until a red precipitate formed. This was collected on Celite and washed thoroughly with cold H_2O (250 mL), cold EtOH (15 mL) and Et_2O (15 mL). The residue was redissolved in CH_3CN and solvent removed in vacuo. [Ru(Phtpy)(**4**)][PF_6]$_2$ was isolated as a red powder (200 mg, 0.192 mmol, 93%). ^{1}H NMR (400 MHz, CD_3CN) ∂/ppm 9.06 (d, J_{PH} = 11 Hz, 2H, H^{F3}), 8.99 (s, 2H, H^{B3}), 8.68 (m, 4H, H^{A3+E3}), 8.20 (m, 2H, H^{C2}), 7.90 (m, 4H, H^{A4+E4}), 7.76 (m, 2H, H^{C3}), 7.68 (m, 1H, H^{C4}), 7.39 (m, 4H, H^{A6+E6}), 7.15 (m, 4H, H^{A5+E5}), 4.05 (m, 2H, $H^{CH2(Et)}$), 1.31 (t, *J* = 7.0 Hz, 3H, $H^{CH3(Et)}$). ^{13}C {^{1}H} NMR (126 MHz, CD_3CN) ∂/ppm 159.3 (C^{E2}), 158.8 (C^{A2}), 156.2 (C^{B2}), 155.7 (d, J_{PC} = 12 Hz, C^{F2}), 153.7 ($C^{A6/E6}$), 153.3 ($C^{A6/E6}$), 149.2 (C^{B4}), 139.0 (C^{A4+E4}), 137.9 (C^{C1}), 131.3 (C^{C4}), 130.6 (C^{C3}), 128.7 (C^{C2}), 128.5 ($C^{A5/E5}$), 128.2 ($C^{A5/E5}$), 126.4 (d,

J_{PC} = 20 Hz, C^{F3}), 125.6 ($C^{A3/E3}$), 125.4 ($C^{A3/E3}$), 122.5 (C^{B3}), 61.8 ($C^{CH2(Et)}$), 17.5 ($C^{CH3(Et)}$) (C^{F4} not resolved). IR (solid, ν/cm^{-1}) 3315 (br m), 1662 (w), 1605 (w), 1542 (w), 1473 (w), 1412 (m), 1392 (m), 1345 (m), 1289 (w), 1209 (m), 1162 (w), 1140 (m), 1078 (m), 1034 (m), 962 (w), 898 (w), 826 (s), 791 (s), 764 (s), 733 (m), 689 (s), 664 (m), 603 (m). ESI-MS (MeCN): *m/z* 751.4 $[M - H - 2PF_6]^+$ (100%, calc. 751.1). HR ESI-MS *m/z*: 376.0621 $[M - 2PF_6]^{2+}$ (base peak, calc. 376.0619), 751.1172 $[M - H - 2PF_6]^+$ (calc. 751.1165). UV/VIS λ / nm (MeCN, 2.88 × 10^{-5} mol dm^{-3}) (ε / dm^3 mol^{-1} cm^{-1}) 274 (59000), 280 sh (54500), 310 (63000), 330 sh (34000), 485 (23000). Emission (MeCN, 3 × 10^{-5} mol dm^{-3}, λ_{ex} = 485 nm): λ_{em} = 647 nm.

Satisfactory elemental analysis could not be obtained (see text).

[Ru(pytpy)(4)][PF$_6$]$_2$

The method was as for [Ru(Phtpy)(**4**)][PF$_6$]$_2$ starting with pytpy (160 mg, 0.52 mmol) and [Ru(**3**)Cl$_3$] (300 mg, 0.52 mmol). [Ru(pytpy)(**4**)][PF$_6$]$_2$ was isolated as a red powder (130 mg, 0.125 mmol, 24%). ^{1}H NMR (500 MHz, CD_3CN) ∂/ppm 9.05 (d, J_{PH} = 11 Hz, 2H, H^{F3}), 9.03 (s, 1H, H^{B3}), 8.95 (m, 2H, H^{C2}), 8.64 (d, *J* = 7.9 Hz, 2H, $H^{A3/E3}$), 8.61 (d, *J* = 8.1 Hz, 2H, $H^{A3/E3}$), 8.12 (m, 2H, H^{C3}), 7.94 (m, 2H, $H^{A4/E4}$), 7.88 (m, 2H, $H^{A4/E4}$), 7.42 (d, *J* = 6.7 Hz, 2H, $H^{A6/E6}$), 7.35 (d, *J* = 6.7 Hz, 2H, H^{E6}), 7.18 (m, 2H, $H^{A5/E5}$), 7.15 (m, 2H, $H^{A5/E5}$), 4.05 (m, 2H, $H^{CH2(Et)}$), 1.32 (t, *J* = 6.8 Hz, 3H, $H^{CH3(Et)}$). ^{13}C {^{1}H} NMR (126 MHz, CD_3CN) ∂/ppm 158.7 (C^{E2}), 158.5 (C^{A2}), 158.0 (C^{F2}), 157.0 (C^{B2}), 153.8 ($C^{A6/E6}$), 153.7 ($C^{A6/E6}$), 151.5 (C^{C2}), 145.3 (C^{B4+C4}), 139.3 (C^{A4+E4}), 128.8 ($C^{A5/E5}$), 128.6 ($C^{A5/E5}$), 126.2 (d, $J_{PC} \approx$ 20 Hz, C^{F3}), 126.1 ($C^{A3/E3}$), 126.0 ($C^{A3/E3}$), 123.2 (C^{B3}), 123.1 (C^{C3}), 63.2 ($C^{CH2(Et)}$), 17.2 ($C^{CH3(Et)}$) (C^{F4} not

resolved). IR (solid, ν/cm^{-1}) 3350 (br s), 1660 (w), 1599 (s), 1532 (w), 1475 (m), 1394 (m), 1352 (w), 1291 (w), 1202 (s), 1166 (w), 1075 (m), 1069 (m), 1038 (m), 1028 (s), 942 (m), 844 (s), 826 (s), 818 (s), 784 (m), 776 (m), 745 (m). ESI-MS (CH_3CN): *m/z* 376.5 $[M - 2PF_6]^{2+}$ (calc. 376.6). HR ESI-MS *m/z*: 376.5600 $[M - 2PF_6]^{2+}$ (base peak, calc. 376.5595), 752.1135 $[M - H - 2PF_6]^{+}$ (calc. 752.1117). UV/VIS λ / nm (CH_3CN, 1×10^{-5} mol dm^{-3}) (ε / dm^3 mol^{-1} cm^{-1}) 273 (54700), 282 sh (42000), 311 (50300), 331 sh (33000), 486 (21000). Emission (CH_3CN, 3.84×10^{-5} mol dm^{-3}, λ_{ex} = 486 nm): λ_{em} = 704 nm. Found: C, 42.94; H, 3.76; N, 10.33; $C_{37}H_{30}F_{12}N_7O_3P_3Ru \cdot H_2O \cdot 1.5CH_3CN$ (1122.60) requires C, 42.81; H, 3.28; N, 10.16%.

[Ru(1)(4)][PF$_6$]$_2$

The method was as for [Ru(Phtpy)(**4**)][PF$_6$]$_2$ starting with **1** (71 mg, 0.19 mmol) and [Ru(**3**)Cl$_3$] (112 mg, 0.19 mmol). [Ru(**1**)(**4**)][PF$_6$]$_2$ was isolated as a red powder (177 mg, 0.161 mmol, 83%). ^{1}H NMR (400 MHz, CD_3CN) ∂/ppm 9.15 (d, *J* = 1.4 Hz, 1H, $H^{B3/B5}$), 9.12 (d, J_{PH} = 10. Hz, 2H, H^{F3}), 9.08 (d, J = 1.2 Hz, 1H, H^{D3}), 9.05 (d, *J* = 1.4 Hz, 1H, $H^{B3/B5}$), 8.72 (d, *J* = 8.2 Hz, 2H, H^{E3}), 8.66 (d, *J* = 7.9 Hz, 1H, H^{A3}), 8.24 (m, 2H, H^{C2}), 7.94 (td, *J* = 7.9, 1.5 Hz, 1H, H^{A4}), 7.89 (td, *J* = 7.9, 1.5 Hz, 2H, H^{E4}), 7.77 (m, 2H, H^{C3}), 7.69 (m, 1H, H^{C4}), 7.63 (d, *J* = 5.8 Hz, 1H, H^{D6}), 7.56 (dd, *J* = 5.8, 1.8 Hz, 1H, H^{D5}), 7.44 (d, *J* = 5.5 Hz, 1H, H^{A6}), 7.39 (dd, *J* = 5.6, 1.4 Hz, 2H, H^{E6}), 7.18 (m, 1H, H^{A5}), 7.13 (ddd, *J* = 7.7, 5.6, 1.3 Hz, 2H, H^{E5}), 4.07 (m, 2H, $H^{CH2(Et)}$), 3.90 (s, 3H, H^{OMe}), 1.29 (t, *J* = 7.0 Hz, 3H, $H^{CH3(Et)}$). ^{13}C {^{1}H} NMR (126 MHz, CD_3CN) ∂/ppm 165.0 ($C^{C=O}$), 160.6 (C^{D2}), 159.5 (C^{E2}), 159.0 (C^{A2}), 156.4 (C^{B2}), 156.0 (C^{B6}), 154.7 (C^{D6}), 155.6 (d, J_{PC} = 14 Hz, C^{F2}), 153.7 (C^{A6}), 153.3 (C^{E6}), 149.4 (C^{B4}), 139.4 (C^{D4}),

139.2 (C^{A4+E4}), 137.6 (C^{C1}), 131.4 (C^{C4}), 130.6 (C^{C3}), 129.0 (C^{C2}), 128.6 (C^{A5+E5}), 128.2 (C^{D5}), 127.6 (d, J_{PC} = 10 Hz, C^{F3}), 126.8 (C^{E3}), 126.5 (C^{A3}), 125.1 (C^{D3}), 124.0 ($C^{B3/B5}$), 123.7 ($C^{B3/B5}$), 62.1 ($C^{CH2(Et)}$), 54.3 (C^{OMe}), 17.5 ($C^{CH3(Et)}$) (C^{F4} not resolved). IR (solid, ν/cm^{-1}) 3347 (br m), 1722 (w), 1605 (w), 1363 (m), 1268 (w), 1165 (w), 1137 (w), 1075 (w), 1032 (w), 945 (w), 825 (s), 787 (m), 767 (m), 700 (w), 607 (w). ESI-MS (CH_3CN): *m/z* 809.5 [M–H–2PF_6]$^+$ (base peak, calc. 809.1). HR ESI-MS *m/z*: 405.0654 [M – 2PF_6]$^{2+}$ (base peak, calc. 405.0647), 809.1233 [M – H – 2PF_6]$^+$ (calc. 809.1220). UV/VIS λ / nm (CH_3CN, 3.6 × 10^{-5} mol dm^{-3}) (ε / dm^3 mol^{-1} cm^{-1}) 274 (56000), 285 (51500), 309 (57000), 330 sh (41500), 491 (20000). Satisfactory elemental analysis was not obtained (see text).

[Ru(2)(4)][PF_6]$_2$

The method was as for [Ru(Phtpy)(**4**)][PF_6]$_2$ starting with **2** (50 mg, 0.14 mmol) and [Ru(**3**)Cl_3] (78 mg, 0.14 mmol). [Ru(**2**)(**4**)][PF_6]$_2$ was isolated as a red powder (35 mg, 0.032 mmol, 23%). ^{1}H NMR (500 MHz, CD_3CN) ∂/ppm 9.23 (d, J_{PH} = 11.5 Hz, 2H, H^{F3}) overlapping with 9.14 (d, *J* = 1.5 Hz, 1H, $H^{B3/B5}$), 9.12 (d, *J* = 1.3 Hz, 1H, $H^{B3/B5}$), 9.09 (d, *J* = 1.4 Hz, 1H, H^{D3}), 8.98 (m, 2H, H^{C2}), 8.77 (m, 3H, H^{A3+E3}), 8.19 (m, 2H, H^{C3}), 7.98 (td, *J* = 8.1, 1.4 Hz, 1H, H^{A4}), 7.92 (td, *J* = 7.9, 1.5 Hz, 2H, H^{E4}), 7.61 (m, 2H, H^{D5+D6}), 7.46 (d, *J* = 5.6 Hz, 1H, H^{A6}), 7.38 (dd, *J* = 5.7, 1.3 Hz, 2H, H^{E6}), 7.21 (m, 1H, H^{A5}), 7.16 (ddd, *J* = 7.2, 5.6, 1.2 Hz, 2H, H^{E5}), 4.27 (m, 2H, $H^{CH2(Et)}$), 3.91 (s, 3H, H^{OMe}), 1.41 (t, *J* = 6.9 Hz, 3H, $H^{CH3(Et)}$). ^{13}C {^{1}H} NMR (126 MHz, CD_3CN) ∂/ppm 164.3 ($C^{C=O}$), 160.1 (C^{D2}), 159.5 (C^{F2}), 159.3 (C^{E2}), 158.8 (C^{A2}), 157.1 (C^{B2}), 156.5 (C^{B6}), 154.8 (C^{D6}), 153.7 (C^{A6}), 153.4 (C^{E6}), 151.7 (C^{C2}), 146.4 (C^{B4}), 145.2 (C^{C4}),

139.4 (C^{A4}), 139.3 (C^{E4}), 128.6 (C^{A5}), 128.5 (C^{E5}), 127.3 (C^{D5}), 126.4 (d, $J_{PC} \approx$ 10 Hz, C^{F3}), 126.0 (C^{E3}), 125.7 (C^{A3}), 124.4 ($C^{B3/B5}$), 123.3 ($C^{B3/B5}$), 123.0 (C^{D3}), 123.1 (C^{C3}), 62.6 ($C^{CH2(Et)}$), 53.8 (C^{OMe}), 16.9 ($C^{CH3(Et)}$) (C^{F4} and C^{D4} not resolved). IR (solid, ν/cm^{-1}) 3211 (br s), 1729 (m), 1635 (w), 1600 (w), 1475 (w), 1409 (m), 1344 (w), 1313 (m), 1268 (m), 1235 (m), 1165 (m), 1138 (m), 1076 (m), 1030 (m), 950 (m), 826 (s), 786 (s), 753 (m), 688 (m), 652 (m), 605 (m). ESI-MS (MeCN): *m/z* 405.6 $[M - 2PF_6]^{2+}$ (calc. 405.6). HR ESI-MS *m/z*: 405.5628 $[M - 2PF_6]^{2+}$ (base peak, calc. 405.5623), 810.1187 $[M - H - 2PF_6]^{+}$ (calc. 810.1173). UV/VIS λ / nm (CH_3CN, 3.63 × 10^{-5} mol dm^{-3}) (ε / dm^3 mol^{-1} cm^{-1}) 274 (51000), 284 sh (43500), 308 (45000), 330 sh (37000), 491 (18500). Satisfactory elemental analysis could not be obtained (see text).

Crystal structure determination of 1

Data were collected on a Bruker-Nonius Kappa APEX diffractometer; data reduction, solution and refinement used APEX2[21] and SHELX13.[22] Absorption correction was made using the program 'sadabs', as part of the 'scale' package in AEPX2 software.[21] The ORTEP plot was produced with Mercury v. 3.0[23,24] which was also used for structure analysis. $C_{23}H_{17}N_3O_2$, *M* = 367.40, colorless plate, crystal dimensions 0.25 × 0.13 × 0.03 mm, monoclinic, space group $P2_1/c$, *a* = 9.9644(9), *b* = 9.0359(8), *c* = 20.0424(17) Å, β = 96.975(6)^o, U = 1791.2(3) Å^3, Z = 4, D_c = 1.362 Mg m^{-3}, μ(Cu-Kα) = 8.224 mm^{-1}, *T* = 123 K. Total 18887 reflections, 3181 unique, R_{int} = 0.0428. Refinement of 2763 reflections (254 parameters) with $I > 2\sigma(I)$ converged at final $R1$ = 0.0378 ($R1$ all data = 0.0439), $wR2$ = 0.1009

(*wR*2 all data = 0.1048), gof = 1.064. CCDC 983369 contains the supplementary crystallographic data for this paper. These data can be obtained, free of charge, via http://www.ccdc.cam.ac.uk/products/csd/request/ (or from the Cambridge Crystallographic Data Centre, 12 Union Road, Cambridge CB2 1EZ, U.K. (Fax: 44-1223-336033 or e-mail: deposit@ccdc.cam.ac.uk)).

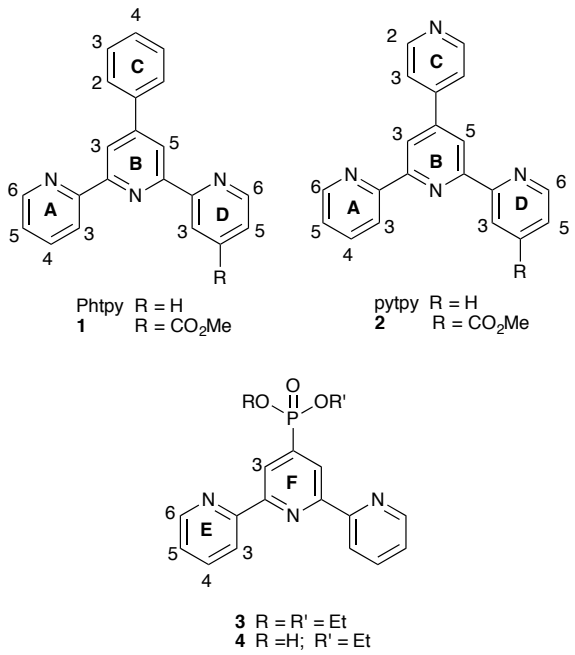

Scheme 1. Structures of ligands **1**–**4** and of Phtpy and pytpy, with atom numbering used for NMR spectroscopic assignments; when R = H, ring A = ring D.

Results and discussion

Synthesis and characterization of ligands 1 and 2

Compounds **1** and **2** (Scheme 1) are the 4'-phenyl and 4'-(4-pyridyl) analogues of 4'-tolyl-2,2':6',2''-terpyridine, the preparation and homoleptic ruthenium(II) complex of which were reported a decade ago by Potvin and

317 coworker.[25] Scheme 2 shows the Kröhnke synthesis of **1** and **2** which
318 yielded the compounds in 33 and 89%, respectively, as white solids. In the
319 electrospray mass spectrum of **1**, the base peak (*m/z* = 338.0) arises from
320 the $[M+H]^+$ ion, and a lower intensity peak at *m/z* = 390.0 was assigned to
321 $[M+Na]^+$. Corresponding peaks at *m/z* 369.2 and 391.1 in the mass spectrum
322 of **2** were also observed. The ^1H and ^{13}C NMR spectra of **1** and **2** were fully
323 assigned with COSY, HMQC and HMBC techniques and were consistent with
324 the inequivalence of the outer pyridine rings of the tpy domain (Scheme 1)
325 and the presence of the ester group.
326

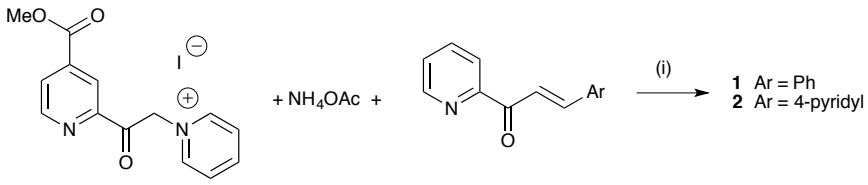

327
328

329 Scheme 2. Synthetic route to ligands **1** and **2**. Conditions: (i) MeOH, reflux.

330

331 Single crystals of **1** were grown by slow evaporation from a $CHCl_3$ solution of
332 the compound and the structure (Figure 1) was confirmed by X-ray
333 diffraction. Important bond parameters are given in the figure caption. The
334 tpy unit adopts a *trans,trans*-conformation, which is expected for a non-
335 protonated ligand. The tpy domain is essentially planar (the angles between
336 the least squares planes through the rings containing N1/N2 and N2/N3 =
337 5.5 and 4.5°); the phenyl ring is twisted 27.6° with respect to the pyridine
338 ring to which it is attached, consistent with minimizing H...H repulsions
339 between the two rings. The dominant packing interactions are (i) face-to-

face π-stacking of tpy domains across inversion centres, (ii) $H_{methyl}...N_{pyridine}$ contacts (H23A...N1^{i} = 2.98, H23B...N1^{i} = 2.81 Å, symmetry code i = 1+*x*, 1+*y*, *z*), and (iii) $N_{pyridine}...HC$ contacts (N3...H3A^{ii}–C3^{ii} = 2.57 Å, symmetry code ii = x, $^{3}/_{2} - y$, $^{1}/_{2} + z$).

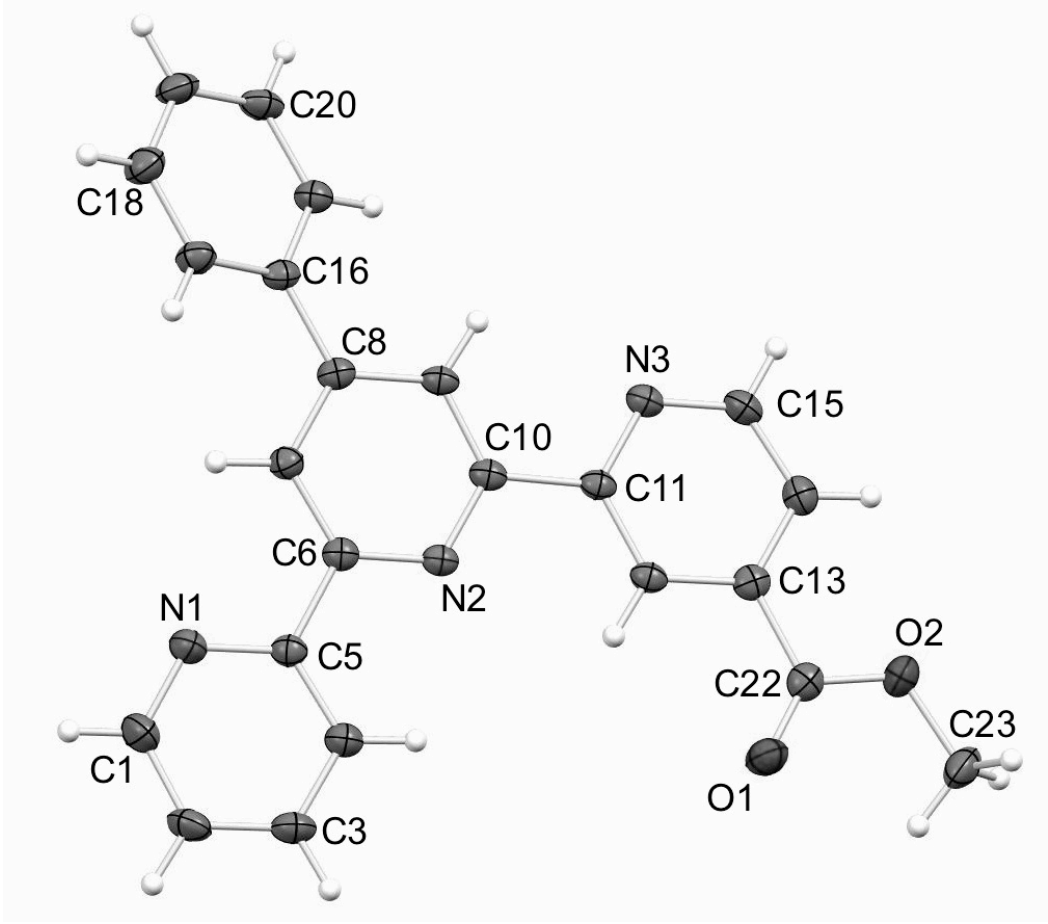

Fig. 1. ORTEP representation of the structure of **1** (ellipsoids plotted at 50% probability level). Selected bond parameters: N1–C1 = 1.342(2), N1–C5 = 1.3386(19), N2–C6 = 1.3415(18), N2–C10 = 1.3412(17), N3–C11 = 1.3463(17), N3–C15 = 1.3295(19), C13–C22 = 1.4993(19), O1–C22 = 1.2052(18), C22–O2 = 1.3309(18), O2–C23 = 1.4524(18) Å; C5–N1–C1 = 117.26(13), C6–N2–C10 = 117.72(12), C15–N3–C11 = 117.80(12), O1–C22–

O2 = 124.63(13), O1–C22–C13 = 124.21(13), O2–C22–C13 = 111.15(12), C22–O2–C23 = 117.15(12)°.

The diethylphosphonate-functionalized ligand **3** has previously been reported by Grätzel and coworkers.[20] The literature synthesis (which gives **3** in 72.3% yield) involves the [$Pd(PPh_3)_4$] catalysed reaction of 4'-bromo-2,2':6',2''-terpyridine with diethyl phosphite in NEt_3 (95 °C for 3 h) followed by dissolution of the mixture in MeOH and chromatographic workup. We adopted the more convenient strategy shown in Scheme 2. The 4'-triflate-functionalized tpy was readily prepared according to the route described by Potts et al,[19] and diethylphosphonate for triflate substitution occurs under microwave conditions to give **4** in 84% yield. The NMR spectroscopic data for **4** were consistent with those published.[20]

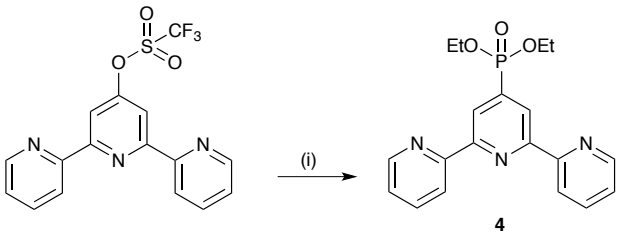

Scheme 3. Synthesis of phosphonate **4**. Conditions: (i) [$Pd(PPh_3)_4$], NEt_3, $HP(O)(OEt)_2$, MeCN, 140 °C, 30 min.

Synthesis and characterization of heteroleptic ruthenium(II) complexes

The heteroleptic complexes discussed in this section are summarized in Scheme 4. Heteroleptic $[Ru(Xtpy)(Ytpy)]^{2+}$ complexes are typically prepared by first preparing an insoluble, paramagnetic ruthenium(III) complex $[Ru(Xtpy)Cl_3]$, and treating this crude material with Ytpy in the presence of *N*-ethylmorpholine which acts as a reducing agent.[26] The precursor for the formation of the new ruthenium(II) complexes was $[Ru(\mathbf{3})Cl_3]$, prepared by reaction of $RuCl_3{\cdot}3H_2O$ with compound **3** in MeOH under reflux. $[Ru(\mathbf{3})Cl_3]$ was isolated as a brown solid.

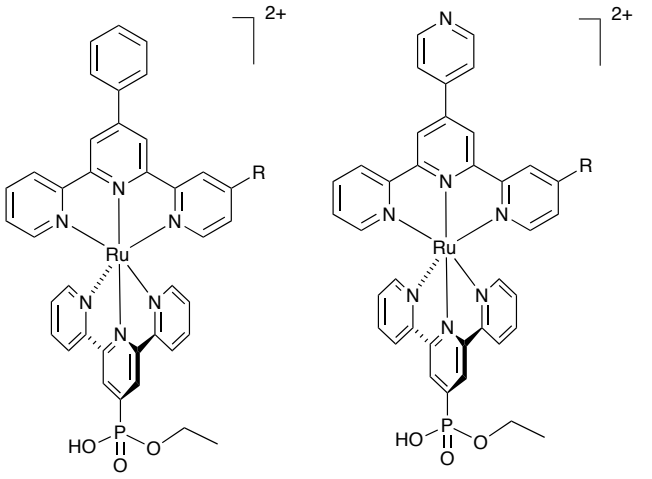

$[Ru(Phtpy)(\mathbf{4})]^{2+}$ R = H
$[Ru(\mathbf{1})(\mathbf{4})]^{2+}$ R = CO_2Me

$[Ru(pytpy)(\mathbf{4})]^{2+}$ R = H
$[Ru(\mathbf{2})(\mathbf{4})]^{2+}$ R = CO_2Me

Scheme 4. Structures of the heteroleptic complex cations prepared as hexafluoridophosphate salts.

Model compounds containing Phtpy and pytpy (Scheme 1) were first prepared by reaction of $[Ru(\mathbf{3})Cl_3]$ with Phtpy and pytpy in the presence of *N*-ethylmorpholine. After anion exchange and chromatographic workup, followed by a second anion exchange (to remove $[NO_3]^-$ introduced from aqueous KNO_3 in the eluant), the ruthenium(II) salts were isolated as red solids. Electrospray mass spectrometic and NMR spectroscopic data were

consistent with the isolated products being complexes of the monoester **4** (Scheme 2) rather than the diester **3**. Partial hydrolysis of **3** during synthesis of ruthenium(II) complexes is known to occur under conditions of high temperature reflux[20] or heating in DMF at 60 ^{o}C.[27] The second hydrolysis step to the phosphonic acid needs acidic conditions or treatment with Me_3SiBr. The ESI mass spectrum of [Ru(Phtpy)(**4**)][PF_6]$_2$ showed the base-peak envelope at m/z 751.4 with an appropriate isotope pattern for the ion [M – H – 2PF_6]$^+$. The loss of H^+ is consistent with the presence of the acidic P–OH group. The high resolution ESI (HR-ESI) mass spectrum was also recorded and peaks arising from [M – H – 2PF_6]$^+$ and [M – 2PF_6]$^{2+}$ confirmed the identity of [Ru(Phtpy)(**4**)]$^{2+}$. The HR-ESI mass spectrum of [Ru(pytpy)(**4**)][PF_6]$_2$ exhibited peak envelopes arising from the [M – H – 2PF_6]$^+$ and [M – 2PF_6]$^{2+}$ ions, and the latter was also observed in the ESI mass spectrum.

The ^{1}H and ^{13}C NMR spectra of CD_3CN solutions of [Ru(Phtpy)(**4**)][PF_6]$_2$ and [Ru(pytpy)(**4**)][PF_6]$_2$ were consistent with the presence of two tpy environments in each complex. A representative spectrum is shown in Figure 2. Spectra were assigned using 2D methods (COSY, HMQC and HMBC); 400 MHz ^{1}H spectra were routinely recorded for better resolution of signals and 500 MHz ^{1}H for 2D measurements. The most characteristic feature of the spectrum in Figure 2 is the appearance of a singlet for protons H^{B3} (Phtpy ligand) and a doublet for the corresponding protons H^{F3} (ligand **4**) arising from ^{31}P-^{1}H coupling (11 Hz). For [Ru(Phtpy)(**4**)][PF_6]$_2$, signals at ∂ 4.05 and 1.31 ppm in the ^{1}H NMR spectrum and their relative integrals with respect to resonances in the

aromatic region were consistent with the monoester **4**; in the ^{13}C NMR spectrum, corresponding signals at ∂ 61.8 and 17.5 ppm were observed.

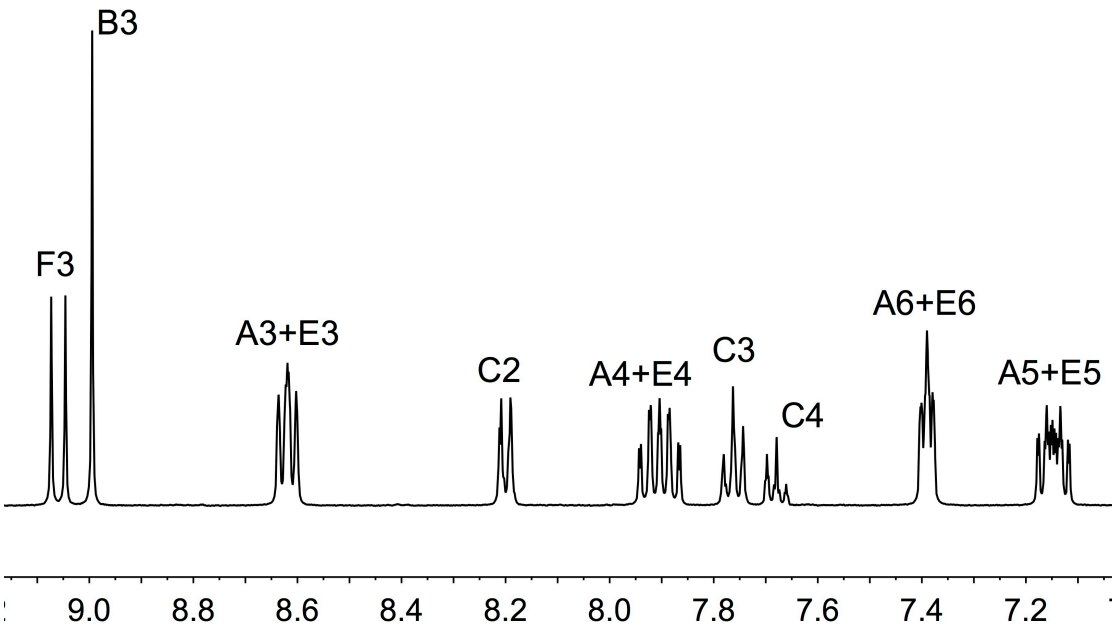

Fig. 2 Aromatic region of the 400 HMz ^{1} H NMR spectrum of [Ru(Phtpy)(**4**)][PF_6]$_2$. See Scheme 1 for ring labelling.

The preparations of [Ru(**1**)(**4**)][PF_6]$_2$ and [Ru(**2**)(**4**)][PF_6]$_2$ were carried out in an analogous manner to those of [Ru(Phtpy)(**4**)][PF_6]$_2$ and [Ru(pytpy)(**4**)][PF_6]$_2$. The base peak in the ESI mass spectrum of [Ru(**1**)(**4**)][PF_6]$_2$ was assigned to [M – H – 2PF_6]$^+$; for [Ru(**2**)(**4**)][PF_6]$_2$, the main peak envelope arose from [M – 2PF_6]$^{2+}$. High resolution ESI data showed peaks arising from [M – 2PF_6]$^{2+}$ and [M – H – 2PF_6]$^+$ for both complexes. The solution ^{1}H and ^{13}C NMR spectra (assigned by 2D methods) of [Ru(**1**)(**4**)][PF_6]$_2$ and [Ru(**2**)(**4**)][PF_6]$_2$ were consistent with the presence of the symmetrical ligand **4** and one asymmetrical ligand. Figure 3 shows part of the ^{1}H NMR spectrum of [Ru(**2**)(**4**)][PF_6]$_2$. The doublet for H^{F3} (J_{PH} = 11.5 Hz) overlaps with one of the two doublets (J_{HH} 1.3 or 1.5 Hz) arising

from H^{B3} and H^{B5}. Pairs of signals for H^{E3}/H^{A3}, H^{E4}/H^{A4}, H^{E5}/H^{A5} and H^{E6}/H^{A6} with relative integrals 2 : 1 appear for the unsubstituted pyridine rings in ligand **4** and for ligands **1** or **2**, respectively The signal for H^{D3} (J_{HH}= 1.4 Hz) was distinguished from those of H^{B3} and H^{B5} by its COSY signature. The relative integrals for the signals for the ethyl groups in **4** in both complexes were consistent with the monoester.

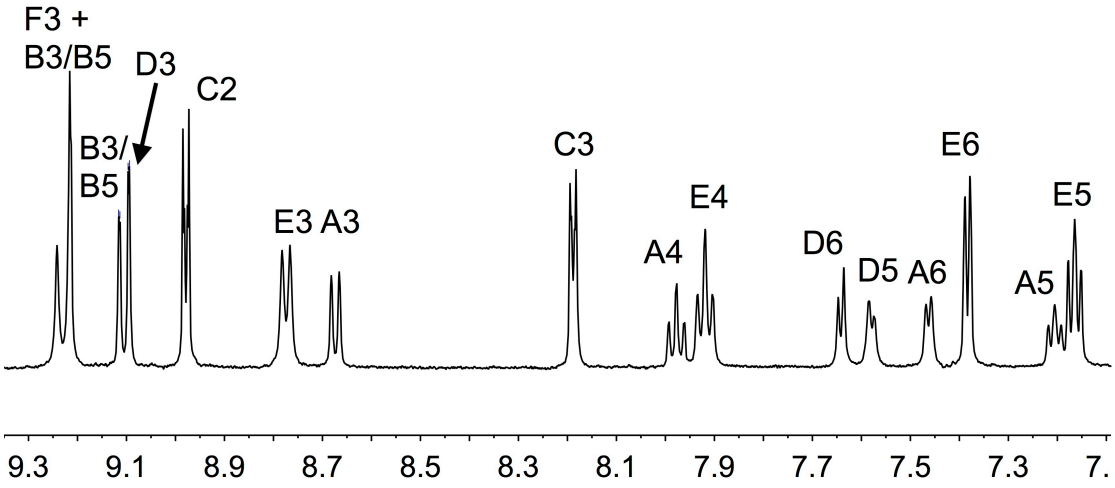

Fig. 3 Aromatic region of the 500 HMz ^{1} H NMR spectrum of [Ru(**2**)(**4**)][PF_6]$_2$. See Scheme 1 for ring labelling.

Yields of [Ru(Phtpy)(**4**)][PF_6]$_2$ and [Ru(**1**)(**4**)][PF_6]$_2$ were >80% yield, but for the complexes containing pytpy, lower yields of ca. 25% were observed, due, in part, to formation of some of the N-protonated species. We noted changes in the ^{1}H NMR spectra which were consistent with protonation of samples in solution. Satisfactory elemental analysis could not always be obtained for the hexafluoridophosphate salts, probably due to small amounts of residual NH_4PF_6. Traces of $[NH_4]^+$ were seen in the ^{1}H NMR spectra (∂ 6.02, $J(^{14}N^{1}H)$ = 53 Hz) of some batches of the complexes. X-ray

quality crystals of solvated [Ru(pytpy)(**4**)][PF_6]$_2$ were obtained, but only preliminary structural data could be obtained because of persistent twinning problems. However, these data were sufficient to confirm the presence of the monoester ligand **4** and the octahedral coordination environment of the ruthenium(II) centre bound by the bis(chelating) donor sets of pytpy and ligand **4**. Despite attempts, X-ray quality single crystals of the other ruthenium(II) complexes were not obtained.

Absorption and emission spectroscopic properties

The absorption spectra of MeCN solutions of the complexes are shown in Figure 4. Each exhibits a series of high-energy bands arising from ligand-based, spin-allowed transitions, and a broad MLCT band in the visible region. The values of λ_{max} for the MLCT absorptions (485–491 nm, see experimental section) compare with 488 nm for both [Ru(Phtpy)$_2$][PF_6]$_2$[26] and [Ru(pytpy)$_2$][PF_6]$_2$.[28] The spectra for [Ru(Phtpy)(**4**)][PF_6]$_2$ and [Ru(pytpy)(**4**)][PF_6]$_2$ are similar to one another and to those of the homoleptic complexes [Ru(Phtpy)$_2$][PF_6]$_2$[26] and [Ru(pytpy)$_2$][PF_6]$_2$.[28] The introduction of the methyl ester substituent leads to a change in the appearance of the absorption maxima (Figure 4), the trend being the same on going from [Ru(Phtpy)(**4**)][PF_6]$_2$ to [Ru(**1**)(**4**)][PF_6]$_2$, and from [Ru(pytpy)(**4**)][PF_6]$_2$ to [Ru(**2**)(**4**)][PF_6]$_2$. The small red-shift in the MLCT band upon introduction of the CO_2Me group is consistent with that observed on going from [Ru(ttpy)$_2$]$^{2+}$ to [Ru(4-MeO_2Cttpy)$_2$]$^{2+}$ (ttpy = 4'-tolyl-2,2':6',2''-terpyridine; 4-MeO_2Cttpy = 4-carboxymethyl-4'-tolyl-2,2':6',2''-terpyridine).[25]

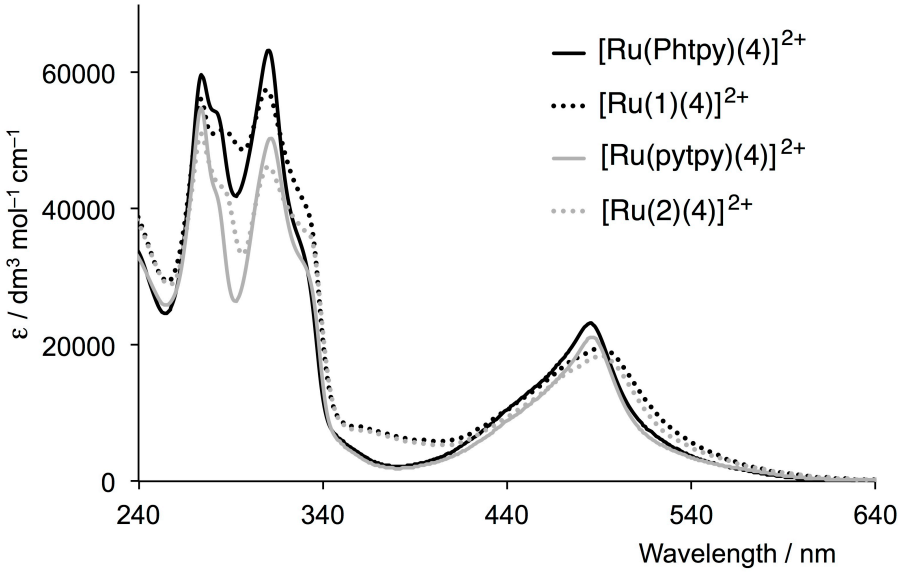

Fig. 4. Absorption spectra of MeCN solutions of [Ru(Phtpy)(**4**)][PF_6]$_2$, [Ru(pytpy)(**4**)][PF_6]$_2$, [Ru(**1**)(**4**)][PF_6]$_2$ and [Ru(**2**)(**4**)][PF_6]$_2$. See experimental section for concentrations.

Excitation into the MLCT band of each of [Ru(Phtpy)(**4**)][PF_6]$_2$ and [Ru(**1**)(**4**)][PF_6]$_2$ (in degassed MeCN at room temperature) gives rise to a weak emission at 647 and 665 nm, respectively, with a quantum yield below the detection limit of the instrument (QY <1%).

Electrochemical properties

The complexes are electrochemically active and cyclic voltammetric data are given in Table 1. The reversible oxidation observed for each complex arises from the Ru^{2+}/Ru^{3+} couple. For the parent [Ru(tpy)$_2$]$^{2+}$, this process occurs at +0.918 V,[26] and introducing electron-donating phenyl groups shifts it to lower potential (+0.895 V in [Ru(Phtpy)$_2$][PF_6]$_2$).[26] Replacing one phenyl substituent by the electron-withdrawing phosphonic ester group shifts the

oxidation to +0.93 V (Table 1). A similar trend is seen on comparing the Ru^{2+}/Ru^{3+} potential in $[Ru(pytpy)_2][PF_6]_2$ (+0.95 V)[28] with that in $[Ru(pytpy)(\mathbf{4})][PF_6]_2$ (+1.01 V). Introduction of the methyl ester unit results in a 0.03 V shift to more positive potential on going from $[Ru(Phtpy)(\mathbf{4})][PF_6]_2$ to $[Ru(\mathbf{1})(\mathbf{4})][PF_6]_2$, or from $[Ru(pytpy)(\mathbf{4})][PF_6]_2$ to $[Ru(\mathbf{2})(\mathbf{4})][PF_6]_2$. This is consistent with the trend observed from $[Ru(ttpy)_2]^{2+}$ to $[Ru(4\text{-}MeO_2Cttpy)_2]^{2+}$.[25] A series of ligand-based reduction processes is observed for each complex (Table 1), consistent with expectations based on related compounds.

Table 1. Cyclic voltammetric data for the ruthenium(II) complexes with respect to Fc/Fc^+ in MeCN solutions with $[^tBu_4N][PF_6]$ as supporting electrolyte, and a scan rate of 0.1 V s^{-1} (ir = irreversible; qr = quasi-reversible).

Complex	$E_{1/2}^{ox}$ / V	$E_{1/2}^{red}$ / V
$[Ru(Phtpy)(\mathbf{4})][PF_6]_2$	+0.93	–1.68, –1.93[qr]
$[Ru(\mathbf{1})(\mathbf{4})][PF_6]_2$	+0.96	–1.49, –1.90, –2.23[ir]
$[Ru(pytpy)(\mathbf{4})][PF_6]_2$	+1.01	–1.57, –2.00[ir]
$[Ru(\mathbf{2})(\mathbf{4})][PF_6]_2$	+1.04	–1.43, –1.85

Conclusions

We have prepared and characterized four new heteroleptic complexes containing $\{Ru(tpy)_2\}$-cores. One ligand contains a phosphonate ester group

designed to act as an anchoring group to metal oxide surfaces. The second ligand is Phtpy or pytpy in the model systems and contains a methyl ester functionality in the second of each pair of complexes. This provides a suitable site for variable functionalization, for example, through transesterification. We plan to use the heteroleptic complexes as a starting point for development of ruthenium(II) dyes suited for sensitization of p-type semiconductors.

Acknowledgements

We thank the Swiss National Science Foundation, the European Research Council (Advanced Grant 267816 LiLo) and the University of Basel for financial support. Sven Brauchli and Dr Heinz Nadig are acknowledged for recording mass spectra. Angelo Lanzilotto is thanked for assistance with absorption spectroscopic measurements.

1 See for example: (a) Sauvage, J.-P.; Collin, J.-P.; Chambron, J. C.; Guillerez, S.; Coudret, C.; Balzani, V.; Barigelletti, F.; De Cola, L.; Flamigni, L. *Chem. Rev*. **1994**, *94*, 993. doi: 10.1021/cr00028a006; (b) Constable, E. C. *Chem. Commun.* **1997**, 1073. doi: 10.1039/A605102B; (c) Baranoff, E.; Collin, J.-P.; Flamigni, L.; Sauvage, J.-P. *Chem. Soc. Rev*. **2004**, *33*, 147. doi: 10.1039/B308983E; (d) Andres, P. R.; Schubert, U. S. *Adv. Mater.* **2004**, *16*, 1043. doi: 10.1002/adma.200306518.

2 Kröhnke, F. *Synthesis*, **1976**, 1. doi: 10.1055/s-1976-23941.

3 Campagna, S.; Puntoriero, F.; Nastasi, F.; Bergamini, G.; Balzani, V. *Topic Curr. Chem.* **2007**, *280*, 117. doi: 10.1007/128_2007_133.

4 Maestri, M.; Armaroli, N.; Balzani, V.; Constable E. C.; Cargil Thompson, A. M. W. *Inorg. Chem.*, **1995**, *34*, 2759. doi: 10.1021/ic00114a039.

5 Grätzel, M. *Inorg. Chem.* **2005**, *44*, 6841. doi: 10.1021/ic0508371.

6 Bozic-Weber, B.; Constable, E. C.; Housecroft, C. E. *Coord. Chem. Rev.* **2013**, *257*, 3089. doi: org/10.1016/j.ccr.2013.05.019.

7 Bozic-Weber, B.; Brauchli, S.; Constable, E. C.; Fürer, S. O.; Housecroft C. E.; Wright, I. A. *Phys. Chem. Chem. Phys*. **2013**, *15*, 4500. doi: 10.1039/C3CP50562F.

8 See for example: (a) Fan, S-Q.; Kim, C.; Fang, B.; Liao, K-X.; Yang, G-J.; Li, C-J.; Kim, J-J.; Ko, J. *J. Phys. Chem. C.* **2011**, *115*, 7747. doi: 10.1021/jp200700e; (b) Wang, S.-W.; Wu, K.-L.; Ghadiri, E.; Lobello, M. G.; Ho, S.-T.; Chi, Y.; Moser, J.-E.; De Angelis, F.; Grätzel, M.; Nazeeruddin, M. K. *Chem. Sci.*, **2013**, *4*, 2423. doi: 10.1039/c3sc50399b; (c) Nguyen, L. H.; Mulmudi, H. K.; Sabba, D.; Kulkarni, S. A.; Batabyal, S. K.; Nonomura, K.; Grätzel, M.; Mhaislkar, S. G. *Phys. Chem. Chem. phys.* **2012**, *14*, 16182. doi: 10.1039/C2CP42959D.

9 He, J.; Lindström, H.; Hagfeldt, A.; Lindquist, S.-E. *Solar Ener. Mater. Solar Cells* **2000**, *62*, 265. doi: org/10.1016/S0927-0248(99)00168-3.

10 Mishra, A.; Fischer, M. K. R.; Bäuerle, P. *Angew. Chem. Int. Ed*. **2009**, *48*, 2474. doi: 10.1002/anie.200804709.

11 Pellegrin, Y.; Le Pleux, L.; Blart, E.; Renaud, A.; Chavillon, B.; Szuwarski, N.; Boujtita, M.; Cario, L.; Jobic, S.; Jacquemin, D.; Odobel, F. *J. Photochem. Photobiol. A*, 2011, 219, 235.

12 Constable E. C.; Homes, J. M. *J. Organomet. Chem*. **1986**, *301*, 203. doi: 10.1016/0022-328X(86)80011-0.

13 Reveco, P.; Cherry, W. R.; Medley, J.; Garber, A.; Gale, R. J.; Selbin, J. *Inorg. Chem*. **1986**, *25*, 1842. doi: 10.1021/ic00231a025.

14 Ji, Z.; Natu, G.; Huang, Z.; Kokhan, O.; Zhang, X. Wu, Y. *J. Phys. Chem. C*, **2012**, *116*, 16854. doi:10.1021/jp303909x.

15 Ji, Z.; Wu, Y. *J. Phys. Chem. C*, **2013**, *117*, 18315 doi: org/10.1021/jp405659m.

16 Eryazici, I.; Moorefield, C. N.; Durmus, S.; Newkome, G. R. *J. Org. Chem*. **2006**, *71*, 1009. doi: 10.1021/jo052036l .

17 Zhao, L.-X.; Kim, T. S.; Ahn, S.-H.; Kim, T.-H.; Kim, E.; Cho, W.-J.; Choi, H.; Lee, C.-S.; Kim, J.-A.; Jeong, T. C. Chang, C.; Lee, E.-S. *Bioorg. Med. Chem. Lett.* **2001**, 11, 2659. doi.org/10.1016/S0960-894X(01)00531-5.

18 Wang, J.; Hanan, G. S. *Synlett* **2005**, *8*, 1251. doi: 10.1055/s-2005-868481.

19 Potts, K. T.; Konwar, D. *J. Org. Chem*. **1991**, *56*, 4815. doi: 10.1021/jo00015a050.

20 Zakeeruddin, S. M.; Nazeeruddin, M.K.; Pechy, P.; Rotzinger, F. P.; Humphry-Baker, R.; Kalyanasundaram, K.; Grätzel, M. *Inorg. Chem.* **1997**, *36*, 5937. doi: 10.1021/ic970008i.

21 Bruker Analytical X-ray Systems, Inc., 2006, APEX2, version 2 User Manual, M86-E01078, Madison, WI.

22 Sheldrick, G. M. *Acta Crystallogr., Sect. A* **2008**, *64*, 112. doi: 10.1107/S0108767307043930

23 Bruno, I. J.; Cole, J. C.; Edgington, P. R.; Kessler, M. K.; Macrae, C. F.; McCabe, P.; Pearson, J.; Taylor, R. *Acta Crystallogr., Sect. B* **2002**, *58*, 389. doi: 10.1107/S0108768102003324.

24 Macrae, C. F.; Bruno, I. J.; Chisholm, J. A.; Edgington, P. R.; McCabe, P.; Pidcock, E.; Rodriguez-Monge, L.; Taylor, R.; van de Streek, J.; Wood, P. A. *J. Appl. Cryst.* **2008**, *41*, 466. doi: 10.1107/S0021889807067908.

25 Mikel C.; Potvin, P. G. *Polyhedron* **2002**, *21*, 49. doi: 10.1016/S0277-5387(01)00959-7

26 Constable, E. C.; Cargill Thompson, A. M. W.; Tocher, D. A.; Daniels, M. A. M. *New J. Chem.* **1992**, *16*, 855. doi: none found.

27 Zhong, D. K.; Zhao, S.; Polyansky, D. E.; Fujita, E. *J. Catalysis*, **2013**, *307,* 140. doi: org/10.1016/j.jcat.2013.07.018.

28 Constable, E. C.; Cargill Thompson, A. M. W. *J. Chem. Soc., Dalton Trans*. **1994**, 1409. doi: 10.1039/DT9940001409.